Chapter 1

Solar Energy Conversion and Noise Characterization in Photovoltaic Devices with Ventilation

Himanshu Dehra

Additional information is available at the end of the chapter

http://dx.doi.org/10.5772/intechopen.79706

Abstract

An investigation is performed on solar energy conversion and noise characterization in photovoltaic devices with ventilation. A parallel plate photovoltaic (PV) device was installed with a pair of PV modules, a ventilated air cavity, and an insulating back panel of plywood board filled with polystyrene installed in an outdoor test room. The characterization of noise interference due to power difference of two intensities for composite waves on a PV device is presented. Standard definitions of noise sources, their measurement equations, their units, and their origins under limiting reference conditions are devised. The experiments were conducted for obtaining currents, voltages, temperatures, air velocities, sensible heat capacity, and thermal storage capacity of a PV device with active ventilation through an outdoor test room. Photovoltaic amplification was attained with power output from a potentiometer through the rotation of its circular knob. A parallel plate PV device was studied for its electrical parameters as resistance-capacitance (RC) electrical analog circuit. The effect of inductive and capacitive heating losses was considered in evaluating electrical characteristics of a PV device exposed to solar radiation. Noise filter systems as per noise sources are illustrated with examples. Some examples of noise unit calculations are tabulated based on devised noise measurement equations.

Keywords: solar energy conversion, PV device, photovoltaic amplification, noise characterization, ventilation, solar energy acoustics

1. Introduction

Solar energy conversion occurs at solar cells, and solar intensity of incident solar energy is converted into electric power and waste heat. The photovoltaic devices with ventilation provide means for converting waste heat lost to surrounding environment into useful thermal

power. The composite waves are transmitted in photovoltaic (PV) devices due to stresses and oscillations of incident solar and ventilation energy. In this way, solar power intensity is converted into heat, fluid, electricity, light, sound, and fire depending on intensities of its transmitted composite waves in PV devices. This chapter has summarized the concept of noise characterization in PV devices with ventilation due to solar energy conversion. The following sections define and describe noise, its sources and its measurement equations with support of experimental and numerical results of a PV device with ventilation. In order to support the noise wave characterization, signal processing is achieved from a PV device composed of RC analog signal. The noise characterization is exemplified with noise filters. Some noise unit calculations deduced from the devised noise measurement equations are also presented.

1.1. Noise

Noise, defined as "a sensation of unwanted intensity of a wave," is perception of a pollutant and a type of environmental stressor. An environmental stressor such as noise may have detrimental effects on various aspects of health. The unwanted intensity of a wave is noise propagation due to transmission of waves (viz. physical agents) such as light, sound, heat, electricity, fluid, and fire. A unified theory for stresses and oscillations is applicable so as to take into effect of all the physical agents as an environmental stressor on a human body [1]. As per the theory, the stresses developed on a particle due to various forces are classified as fundamental stresses, internal stresses, and external stresses. The fundamental stresses are developed due to the presence of gravitational and electromagnetic forces of a solar system. The internal stresses are developed under the influence of fundamental stresses and are defined by properties and composition of a particle. A theory of noise interference in a wave is deemed based on noise sources and their units [1–5]. The noise sources, their measurement equations and units, are derived from the concept of interference of waves and unified theory of stresses and oscillations [6–8]. The noise filters are classified as per source signal of unwanted frequencies from solar power, electric power, light power, sound power, heat power, fluid power, and fire power [8–10]. This noise concept is also useful for characterization and checking of a human noise behavior [11].

1.2. Noise characterization

The interference of noise arises due to the difference of power of two intensities. The intensity of power for any particle body is a function of the development of various stresses. The phenomenon of acoustic resonance occurs when critical stress level matches with the natural stress level necessary for the oscillation of a particle body [1, 8]. The criteria for generation of acoustic resonance include waves propagated with transmission of light, sound, noise, heat, electricity, fluid, and fire from a particle body. The sensation and perception of noise from light, sound, heat, electricity, fluid, and fire is a physiological response from the sensory organs of a standard (average) human body [8].

The characterization of noise interference due to difference of power of two intensities is conceptualized. The difference of two power intensities is due to the transmission of light, sound heat, electricity, fluid, and fire into a particle body. The sources of noise are classified

according to the type of wave of interference, such as light, sound, heat, electricity, fluid, and fire. The criteria for definitions of noise are based on areas of energy stored in a wave, due to interference, speed of wave, and difference of power between two intensities of wave.

2. Sources of noise

The sources of noise are classified according to the type of wave of interference [3]:

Light: In the electromagnetic radiation wavelength band from approximately between 380 and 765 nm, the visual sensation of light is tested by the eye of an observer seeing a radiant energy. The physiological response from an average eye defines the units of light. The sensitivity of human eye is not same in all wavelengths or colors. The contribution of adding daylight is visual sensation in the visible region of the solar energy spectrum.

Sound: In the range of frequencies between 20 and 20,000 Hz, the sound is evaluated due to the presence of fluid pressure energy as a hearing sensation by the ear. The sound units are based on the functional feedback of an average ear. The sensitivity of sound to the whole frequency band is not the same for human ear.

Heat: In the electromagnetic radiation between 0.1 and 100 μm, the heat as a temperature sensation is examined by the human body. The sensation function of temperature defines the units of heat. The temperature sensation function is a measure of coldness and hotness. The comfort zone of temperature is evaluated from functional feedback of a human body which also defines the thermal comfort. The contribution to discomfort of human body is in the ultraviolet region of solar energy spectrum.

Electricity: With passing of direct current or an alternating current, the electricity as a shock sensation is evaluated by skin of an observer due to the electromagnetic energy stored in a conductor which is short circuited by a human body.

Fluid: The fluid as combined ventilation and breathing sensation is evaluated by the amount of fluid passed either externally or internally through a standard (average) human body.

Fire: The exposure of radiant energy and fluid acting on the skin surface of an average human body defines the fire as a sensation of burning.

3. Definitions

The definitions of noise sources are characterized by energy area stored in a wave with its speed and difference due to power intensities of two waves due to the interference [8].

Noise of sol: The difference of power intensities between two solar power systems causes noise of sol (S). The power storage on a unit area per unit time defines the amplitude of a solar energy wave.

The storage of solar power is defined by a solar energy wave pack of unit cross sectional area and of length s, the velocity of light.

Noise of therm: The difference of power intensities between two heat power systems causes noise of therm. The power storage on a unit area per unit time defines the amplitude of a heat wave.

The storage of heat power is defined by the heat energy wave pack of unit cross sectional area and of length s, the velocity of light.

Noise of photons: The difference of power intensities between two lighting power systems causes noise of photons. The power storage on a unit area per unit time defines the amplitude of a light beam.

The storage of light beam is defined by the light beam packet of unit cross sectional area and of length s, the velocity of light.

Noise of electrons: The difference of power intensities between two electrical power systems causes noise of electrons. The power storage on a unit area per unit time defines the amplitude of an electricity wave.

The storage of electrical power is defined by an electricity wave pack of unit cross sectional area and of length s, the velocity of light.

Noise of scattering: The difference of power intensities between two fluid power systems causes noise of scattering. The power storage on a unit area per unit time defines the amplitude of a fluid wave.

The storage of fluid power is defined by the fluid energy wave pack of unit cross sectional area and of length s, the velocity of fluid.

Noise of scattering and lightning: The difference of power intensities between two fire power systems causes noise of scattering and lightning. The power storage on a unit area per unit time defines the amplitude of a fire flash.

The storage of fire power of light is defined by the fire pack of unit cross sectional area and of length s, the velocity of light. The storage of fire power of fluid is defined by the fire pack of unit cross sectional area and of length s, the velocity of fluid.

Noise of elasticity: The difference of power intensities between two sound power systems causes noise of elasticity. The power storage on a unit area per unit time defines the amplitude of a sound wave. The storage of sound power is defined by the sound energy wave pack of unit cross sectional area and of length s, the velocity of sound.

4. Noise measurement equations

The following standard measurement equations are derived and adopted from the standard definitions for sources of noise interference as mentioned in previous sections [8, 9].

Noise of sol: For a pack of solar energy wave, the multiplication of solar power storage and the velocity of light give solar power intensity I. On taking logarithm of two intensities of solar power, I_1 and I_2, provides intensity difference. It is mathematically expressed as [8]:

$$Sol = \log(I_1)(I_2)^{-1} \tag{1}$$

But, the logarithmic unit ratio for noise of sol is expressed as *Sol*. The oncisol (oS) is more convenient for solar power systems. The mathematical expression by the following equality gives an oncisol (oS), which is 1/11th unit of a *Sol* [8]:

$$oS = \pm 11 \log(I_1)(I_2)^{-1} \tag{2}$$

Noise of therm: For a pack of heat energy wave, the multiplication of the total power storage and the velocity of light gives heat power intensity I. The pack of solar energy wave and heat energy wave (for the same intensity I) have same energy areas; therefore, their units of noise are the same as *Sol*.

Noise of photons: For a pack of light energy beam, the multiplication of the total power storage and the velocity of light gives light power intensity I. The pack of solar energy wave and light energy beam (for the same intensity I) have same energy areas; therefore, their units of noise are the same as *Sol*.

Noise of electrons: For a pack of electricity wave, the multiplication of the total electrical storage and the velocity of light gives electrical power intensity I. The pack of solar energy wave and electricity wave (for the same intensity I) have same energy areas; therefore, their units of noise are the same as *Sol*.

Noise of scattering: For a pack of fluid energy wave, the multiplication of the total power storage and the velocity of fluid gives fluid power intensity I. On taking logarithm of two intensities of fluid power, I_1 and I_2, provides intensity difference. It is mathematically expressed as [8]:

$$Sip = \log(I_1)(I_2)^{-1} \tag{3}$$

But, the logarithmic unit ratio for noise of scattering is *Sip*. The oncisip (oS) is more convenient for fluid power systems.

The mathematical expression by the following equality gives an oncisip (oS), which is 1/11th unit of a *Sip* [8]:

$$oS = \pm 11 \log(I_1)(I_2)^{-1} \tag{4}$$

For energy area determination for a fluid wave, the water with a specific gravity of 1.0 is the standard fluid considered with a power of ±1 W m^{-2} for a reference intensity I_2.

Noise of scattering and lightning: For a pack of fire wave, the intensity, I, of fire flash with power of light is the multiplication of the total power storage and the velocity of light. Whereas

for a pack of fire wave, the intensity, I, of fire flash with power of fluid is the multiplication of the total power storage capacity and the velocity of fluid.

For a noise due to fire flash, the collective effect of scattering and lightning is to be obtained by the superimposition principle.

- For the same intensity I, the pack of solar energy wave and a fire flash with light power has the same energy areas; therefore, their units of noise are the same as *Sol*. The therm power may also be included in fire flash with power of light.
- For the same intensity I, the pack of fluid energy wave and a fire flash with fluid power has the same energy areas; therefore, their units of noise are same as *Sip*. In determining the areas of energy for the case of fluids other than water, a multiplication factor in specific gravity of fluid is to be considered.

Noise of elasticity: For a pack of sound energy wave, the product of the total power storage and the velocity of sound gives sound power intensity I. On taking logarithm of two intensities of sound power, I_1 and I_2, provides intensity difference. It is mathematically expressed as [8]:

$$Bel = \log(I_1)(I_2)^{-1} \tag{5}$$

But, the logarithmic unit ratio for noise of elasticity is *Bel*. The oncibel (oB) is more convenient for sound power systems. The mathematical expression by the following equality gives an oncibel (oB), which is 1/11th unit of a *Bel* [8]:

$$oB = \pm 11 \log(I_1)(I_2)^{-1} \tag{6}$$

There are following elaborative points on choosing an *onci* as 1/11th unit of noise [11]:

Reference value used for I_2 is −1 W m^{-2} on positive scale of noise and 1 W m^{-2} on negative scale of noise. In a power cycle, all types of wave form one positive power cycle and one negative power cycle (see **Figure 10**). Positive scale of noise has ten positive units and one negative unit, whereas the negative scale of noise has one positive unit and ten negative units:

i. Each unit of sol, sip, and bel is divided into 11 parts, 1 part is 1/11th unit of noise, and

ii. The base of logarithm used in noise measurement equations is 11.

The reference value of I_2 is −1 W m^{-2} with I_1 on positive scale of noise, should be taken with negative noise measurement expression (see Eqs. (2), (4) and (6)); therefore, it gives positive values of noise.

The reference value of I_2 is 1 W m^{-2} with I_1 on negative scale of noise, should be taken with positive noise measurement expression (see Eqs. (2), (4) and (6)); therefore, it gives negative values of noise.

Some noise unit calculation examples are illustrated later in this chapter.

4.1. Limiting conditions and reference values

Table 1 has summarized the units of noise and their limiting conditions [3].

Reference*	Noise scales and limiting conditions		
$I_2 = \pm 1\ W\ m^{-2}$	**Noise of sol**	**Noise of scattering**	**Noise of elasticity**
Units	**Sol**	**Sip**	**Bel**
$I_1 = 1\ W\ m^{-2}$	No positive solar energy	No positive fluid energy	No positive sound energy
$I_1 = 1+ \rightarrow 0\ W\ m^{-2}$	Decreasing solar energy	Decreasing fluid energy	Decreasing sound energy
$I_1 = +ve$	Increasing solar energy	Increasing fluid energy	Increasing sound energy
$I_1 = -1\ W\ m^{-2}$	Negative solar energy	Negative fluid energy	Negative sound energy
	Darkness	Low pressure	Inaudible range
$I_1 = -ve$	Darkness increasing, distance from point source of light increasing	Low pressure increasing, vacuum approaching	Inaudible range increasing, vacuum approaching
$I_1 = -1+ \rightarrow 0\ W\ m^{-2}$	Negative solar energy	Negative fluid energy	Negative sound energy
	Decreasing darkness	Decreasing low pressure	Decreasing inaudible range

*Reference value of $I_2 = \pm 1\ W\ m^{-2}$ signifies the limiting condition with areas of noise interference approaching to zero.

Table 1. Noise under limiting conditions.

5. Noise filter systems

The criteria for definitions of filters for noise filtering are based on the areas of energy stored in a wave due to the noise interference, speed of wave, and difference of power between two intensities of wave [8]. The filtered noise signals are considered from systems of solar power, electric power, light power, sound power, heat power, fluid power, and fire power. The noise filters as per sources of noise are defined as follows [8]:

Filter for noise of sol: This filter is used to filter noise due to the difference of intensities of power between two solar power systems. Example: window curtain, window blind, wall, and sunglasses.

Filter for noise of therm: This filter is used to filter noise due to the difference of intensities of power between two heat power systems. Example: house, insulation, clothing, and furnace.

Filter for noise of photons: This filter is used to filter noise due to the difference of intensities of power between two lighting systems. Example: 3-D vision of any object, electric bulb, television, computer, and LCD screen laptop.

Filter for noise of electrons: This filter is used to filter noise due to the difference of intensities of power between two electrical power systems. Example: AM/FM radio clock with ear phones, telephone instrument with ear phones, and CD audio player with ear phones.

Filter for noise of scattering: This filter is used to filter noise due to the difference of intensities of power between two fluid power systems. Example: electric fan, pump, motor vehicle, river stream, rain, and tap water.

Filter for noise of scattering and lightning: This filter is used to filter noise due to the difference of intensities of power between two fire power systems. Example: lighter, matchstick, gas stove, locomotive engine, and thunderbolt.

Filter for noise of elasticity: This filter is used to filter noise due to the difference of intensities of power between two sound power systems. Example: human vocal chords, organ pipe, thunderbolt, and drum beats.

5.1. Some examples of noise filters

Some examples of noise filters are enumerated as under [10]:

Human voice production: The example of phonetics of filtering sound of a human speech is illustrated. The human speech is synthesized due to the development of stresses at vocal folds. The smoothening of the sound is a function of its amplitude and its shape of oscillations at vocal tract of a human being. The vocal tract is a resonant cavity wall with sound energy stored in oscillations of its vocal folds. The vocal apparatus showing the mechanism of synthesis of human speech is illustrated in **Figure 1**.

An airflow window with a photovoltaic solar wall: The filtering of solar energy is illustrated through an example of an airflow window attached with a shading device. An airflow window is fixed with a movable roller blind to control the transmission of daylight as well as the amount of solar heat. The bottom portion of photovoltaic solar wall is used for controlling the amount of air ventilation along with the generation of solar electric power. The example is illustrated in **Figure 2**.

Psychrometric air conditioner: An elementary air conditioner for summer comfort conditioning consists of a cooling coil, a cooling fluid with a filter. The schematic of operation of a psychrometric air conditioner is illustrated in **Figure 3**.

Telephone line: The impedance of a telephone line is composed of distributed resistance, capacitance, and inductance. The impedance of telephone line is proportional to the insulation, loop length, and whether the wire is buried, aerial or bare parallel wires strung on

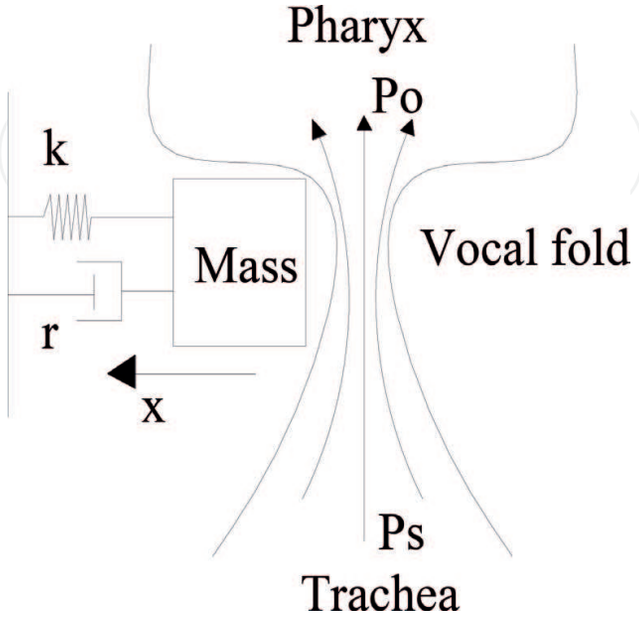

Figure 1. A human vocal mechanism.

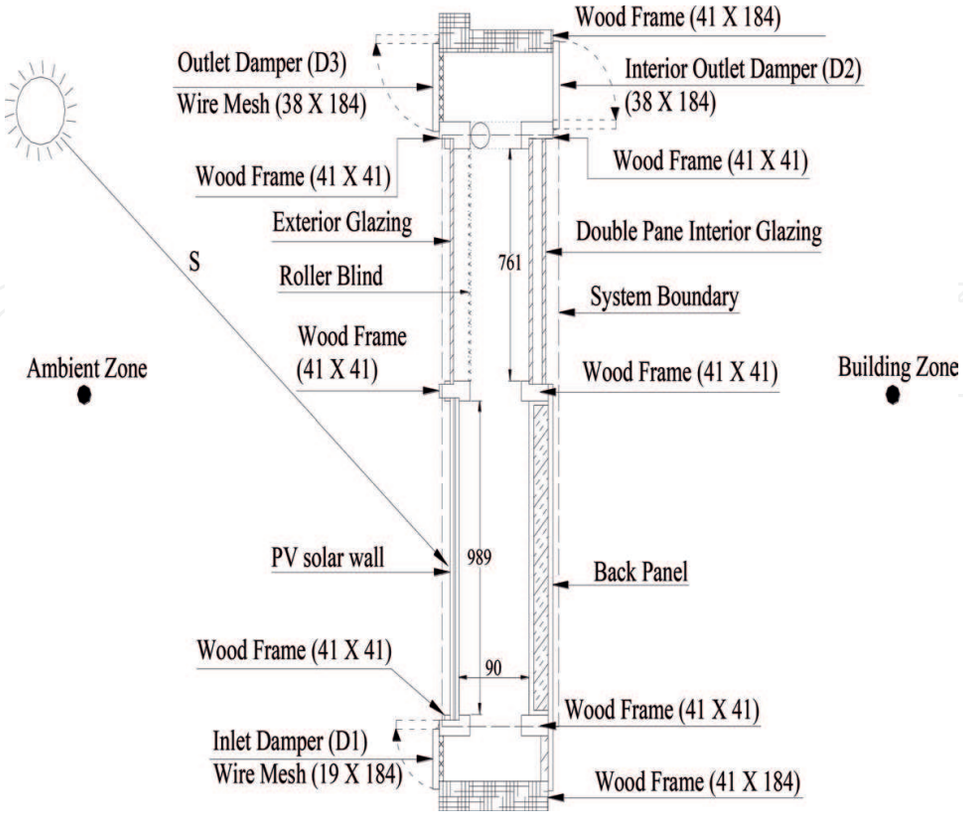

Figure 2. An airflow window with a photovoltaic solar wall (dimensions shown are in mm).

telephone pole. A telephone line is usually supplied with a 48 VDC from the telephone exchange. The schematic of operation of a telephone line with telephone instrument is illustrated in **Figure 4**.

Fire and smoke detection system: A fire detection system consists of a control system with interconnected alarms, smoke, and heat detectors. A fire detector is a device which is used for presetting an alarm at a particular temperature. A smoke detector is a device which is used for presetting an alarm when a certain percentage of smoke accumulates. The photovoltaic cell activates the smoke alarm only if it senses requisite obscuration of light over a unit area with control from BMS. The schematic of various components for fire detection system is illustrated in **Figure 5**.

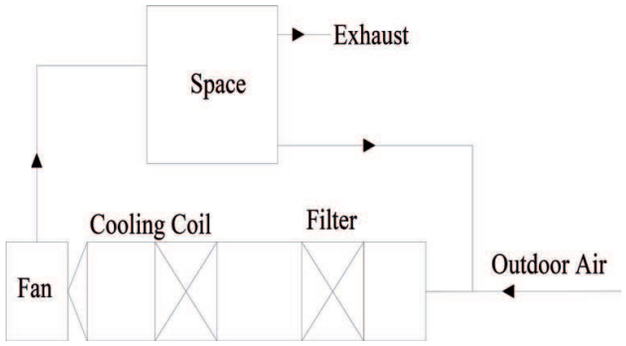

Figure 3. A psychrometric air conditioner.

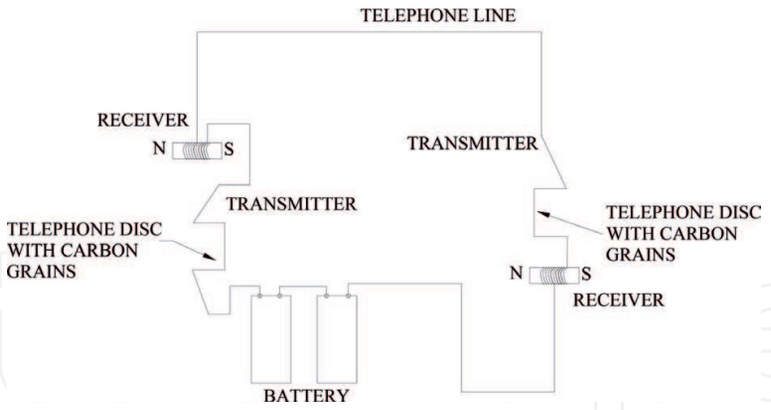

Figure 4. Operation of a telephone line.

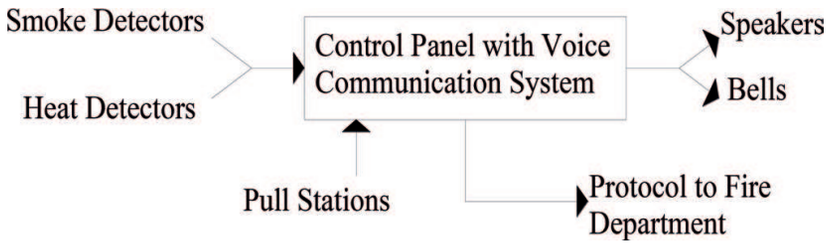

Figure 5. A fire detection system.

6. Experimental and numerical results

The full scale experimental setup for a parallel plate photovoltaic device connected to a potentiometer was installed in an outdoor room facility located at Concordia University, Montréal, Québec, Canada [12–23]. The schematic of the experimental setup is illustrated in **Figure 6**. An amplifier was built with a pair of photovoltaic (PV) modules forming a parallel plate channel with a plywood board and connected to a potentiometer. A potentiometer, a wire-wound variable resistor of up to 50 Ω, was a wire-wound circular coil with a sliding knob contact [23]. It was used to vary electrical resistance across connected PV modules without interrupting the current. The characteristics of a parallel plate photovoltaic device connected to a potentiometer were established by varying electrical resistance with the rotation of knob of a potentiometer. The current-voltage measurements were obtained for determining electric power output with a series electrical circuit connection of a pair of vertically inclined PV modules installed on a wooden frame.

The temperatures were measured as a function of volume of a parallel plate photovoltaic device. The nonlinear thermal results include measurements of temperatures for PV modules, insulating panel, and ventilated air column in the wooden frame. The air velocities were developed in the ventilated air column for the transportation of heat both as a measure of buoyancy and fan induced ventilation. The electrical measurement results of currents, voltages, and power with varying electrical resistance of potentiometer are presented in **Table 2**. The thermal measurement results of temperatures of various components of PV device, ambient air and room air temperatures, air velocities and solar intensities are presented in **Table 3**. The location and nomenclature of sensors are presented in **Table 4**. The results of the power output from a potentiometer with the rotation of circular knob are illustrated in **Figure 7**.

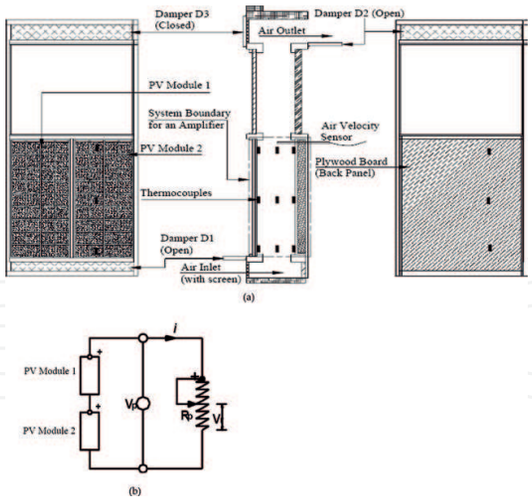

Figure 6. Schematic of experimental setup for a parallel plate photovoltaic device connected to a potentiometer: (a) location of sensors; and (b) electrical circuit diagram.

A simulation model for the prediction of temperature distributions varying with the volume of a parallel plate photovoltaic device was developed. The model was used to predict the temperature distributions at pre-defined locations in PV module, plywood board, and air flowing through a parallel plate channel through the walls of vertically inclined photovoltaic modules. The model results of the temperature plots are illustrated in **Figure 8(a)–(c)**. Some noise unit examples for an air duct exposed to solar radiation are illustrated in **Tables 5–8**. These tables have shown noise unit calculations on positive scale of noise.

6.1. Photovoltaic amplification

The phenomenon of photovoltaic amplification is observed from the graphs of **Figures 7** and **8** [21]. The gain in steady state electrical and thermal functions for a photovoltaic device is a factor of its volume or resistance. This operational characteristic is similar to the operation of a loudspeaker. The electrical analog is used to describe the resonance phenomenon for

Rotation	Volts	Amps	Watts	Rotation	Volts	Amps	Watts	Rotation	Volts	Amps	Watts
240°	18.7	—	—	83°	16.3	0.935	15.23	30°	9.7	1.577	15.21
239°	16.5	0.331	5.461	75°	16.0	1.014	16.26	27°	9.0	1.587	14.33
201°	17.4	0.414	7.195	69°	15.8	1.100	17.38	21°	7.1	1.583	11.24
185°	17.5	0.454	7.940	64°	15.5	1.165	18.04	18°	6.2	1.573	9.831
162°	17.3	0.513	8.885	55°	15.0	1.302	19.53	17°	5.7	1.578	9.026
150°	17.18	0.550	9.449	50°	14.5	1.386	20.05	12°	3.9	1.567	6.257
142°	17.19	0.582	10.00	43°	13.2	1.503	19.79	10°	3.2	1.553	4.840
128°	17.1	0.640	10.93	42°	13.1	1.493	19.49	1.5°	0.5	1.593	0.807
107°	16.8	0.750	12.51	37°	11.9	1.536	18.26	1°	0.3	1.59	0.426
89°	16.4	0.884	14.45	32°	10.5	1.567	16.42	0°	—	1.643	—

Table 2. Sample electrical measurement results of a PV device with varying resistance of potentiometer.

Run no.	S (W m^{-2})	Ep (W)	To (°C)	Ts (°C)	v (m s^{-1})	T_p(b) (°C)	T_p(m) (°C)	T_p(t) (°C)	T_b(b) (°C)	T_b(m) (°C)	T_b(t) (°C)	T_a(b) (°C)	T_a(m) (°C)	T_a(t) (°C)
1	697.5	31.0	13.5	22.1	0.451	34.5	33.01	36.2	20.2	24.4	27.6	18.7	19.3	22.5
2	725.4	31.1	15.9	22.9	0.362	32.5	33.3	35.7	20.2	23.9	29.1	18.3	19.7	23.3

Table 3. Sample thermo-fluid measurement results.

Locations shown in Figure 1	T_p(b) (°C)	T_p(m) (°C)	T_p(t) (°C)	T_b(b) (°C)	T_b(m) (°C)	T_b(t) (°C)	T_a(b) (°C)	T_a(m) (°C)	T_a(t) (°C)	Air velocity sensor
y (cm)	15	55	94	15	55	94	15	55	94	99
Z (cm)	60	60	60	60	60	60	60	60	60	60
X (mm)	6.2	6.2	6.2	96.2	96.2	96.2	51.2	51.2	51.2	51.2

Note: x is horizontal; y is vertical; and z is adjacent 3rd axis of x-y plane.

Table 4. Nomenclature and location of sensors.

equivalent mechanical, hydraulic, and thermal systems of a parallel plate photovoltaic device connected to a potentiometer. **Figure 9(a)** and **(b)** shows series and parallel cases of L-C-R arrangement of resonance, respectively.

6.2. Signal processing: electrical parameters for a PV device

The sinusoidal steady-state response was applied in performing the analysis of the parallel plate PV device circuit, because of the advantage of representing a periodic function in terms of a sinusoidal exponential function. Electrical analog RC circuit parameters of a parallel plate PV device are enumerated as under [2, 13]:

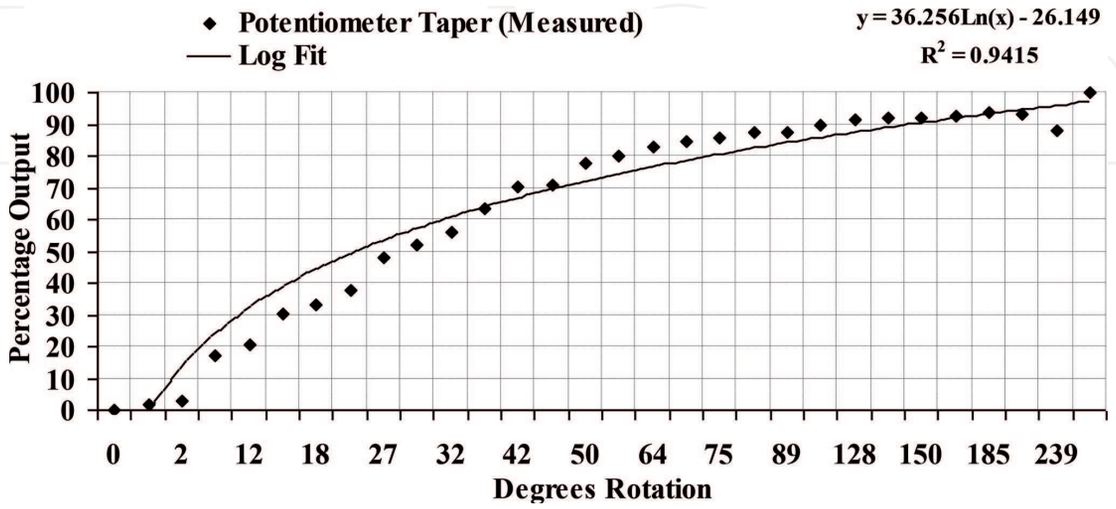

Figure 7. Potentiometer taper (measured) with percentage voltage output.

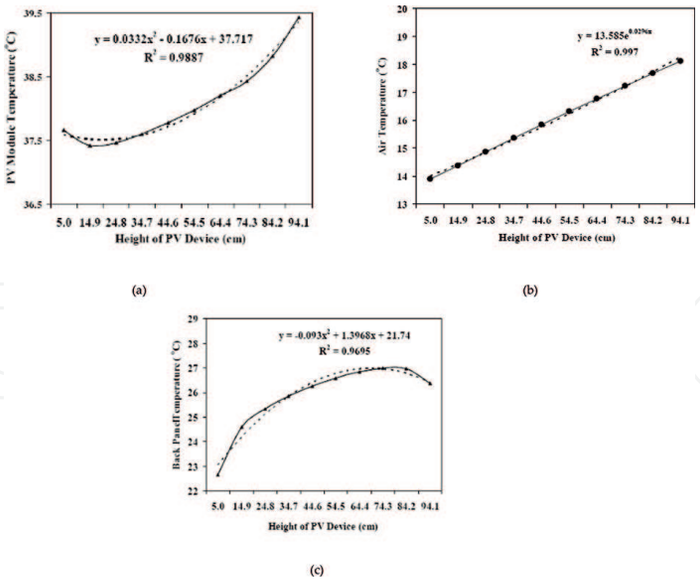

Figure 8. Temperature plots with height of a PV device: (a) PV module; (b) air; and (c) plywood board.

Solar irradiation (W m^{-2})	Air temperature difference (ΔT) (°C)	Noise of Sol oS (oncisol)
450	15.50	28
550	18.90	28.93
650	22.40	29.7
750	25.90	30.36
850	29.40	30.91

Table 5. Temperature difference and noise of sol with solar irradiation (air velocity: 0.75 m s^{-1}).

Air velocity (m s^{-1})	Fluid power (W m^{-2})	Air temperature difference (ΔT) (°C)	Noise of scattering oS (oncisip)
1.35	47.62	15.28	17.72
1.05	37.0	18.22	16.50
0.75	26.45	22.40	15.02
0.45	15.87	28.15	12.65
0.15	05.29	29.80	07.64

Table 6. Temperature difference and noise of scattering with air velocity (S = 650 W m^{-2}).

Capacitance: The capacitance of a parallel plate PV device with air as a dielectric medium was calculated to be 91.2 picofarads.

(ΔT) °C	Mass flow rate (kg s^{-1})	Thermal power (W m^{-2})	Noise of therm oS (oncisol)	(ΔT) (°C)	Mass flow rate (kg s^{-1})	Thermal power (W m^{-2})	Noise of therm oS (oncisol)
15.50	0.01376	71.09	19.5602	15.28	0.0231	117.65	21.868
18.90	0.01275	80.325	20.119	18.22	0.0171	103.85	21.296
22.40	0.0120	89.6	20.614	22.40	0.0120	89.6	20.614
25.90	0.0115	99.2833	21.043	28.15	8.1 X 10^{-3}	76.0	19.866
29.40	0.0111	108.78	21.505	29.80	6.2 X 10^{-3}	61.59	18.898

Table 7. Mass flow rate and noise of therm with (ΔT) (°C).

Air velocity (m s^{-1})	Fluid power (W m^{-2})	Noise of scattering oS (oncisip)	Sound pressure (N m^{-2})	Sound power intensity (W m^{-2})	Noise of elasticity oB (oncibel)
1.35	47.62	17.72	557.5	752.7	30.36
1.05	37.0	16.50	433.65	455.33	28.05
0.75	26.45	15.02	309.75	232.31	24.97
0.45	15.87	12.65	185.85	83.63	20.24
0.15	05.29	07.64	61.94	09.29	10.12

Table 8. Noise of elasticity with air particle velocity (impedance Z_0 = 413 N s m^{-3} at 20°C).

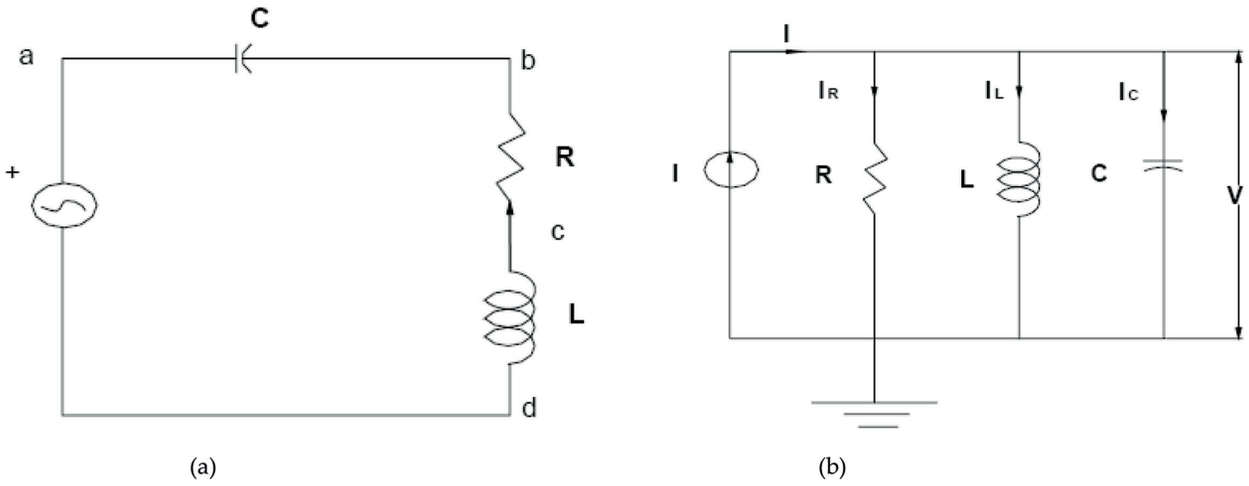

Figure 9. (a) L-C-R series arrangement of resonance and (b) L-C-R parallel arrangement of resonance.

Resistance: The electrical resistances of various components were calculated as: glass coated PV modules were approximated as 5.3 kΩ, air was approximated as 1200 MΩ, and plywood board was approximated as 26.5 Tera Ω. The total equivalent electrical resistance of a parallel plate PV solar wall device was approximated as 5.3 kΩ.

Time constant: The time constant, which is a product of resistance and capacitance, was calculated to be: 0.5 μs. The frequency with this time constant was calculated to be 2 MHz.

Capacitive reactance: The capacitive reactance was calculated to be 872.5 Ω.

Impedance: The impedance of the circuit was calculated to be 5.4 kΩ.

The phase angle θ: The phase angle between capacitance and reactance was calculated to be 9°.

The phasor representation:

$$Z = 5.300 - j0.8725 = 5.4\,\text{k}\Omega \angle -9^{\circ}.$$

Capacitive heating: The joule law gives instantaneous power absorbed by the capacitive impedance which is converted into heat. The heat capacities under critical operation of buoyancy-induced ventilation were calculated to be 59.6, 0.755, and 510.7 for PV module, air, and plywood board, respectively. The total average value of joule heating for the parallel plate PV device was calculated to be 571 kJ.

Induction losses: The induction losses due to the thermal storage effect in the parallel plate PV device were calculated to be 15.9 kJ.

Power factor: The power factor was calculated to be $\cos\theta = 0.911$ lag.

Current function ($i^2(t)$): Using the current function, $i^2(t) = I_m{}^2\sin^2(\omega t + \theta)$, the effective (root mean square) value of current was calculated to be 10.4 amps, and the maximum value of current was calculated to be 14.71 amps.

Voltage function: The voltage function is defined as per the sine wave: $v = V_m\sin(\omega t)$. The effective value of the voltage was calculated to be 60.4 V, and the maximum value of the voltage was calculated to be 85.42 V.

Power function: The instantaneous power is given by the expression [2]:

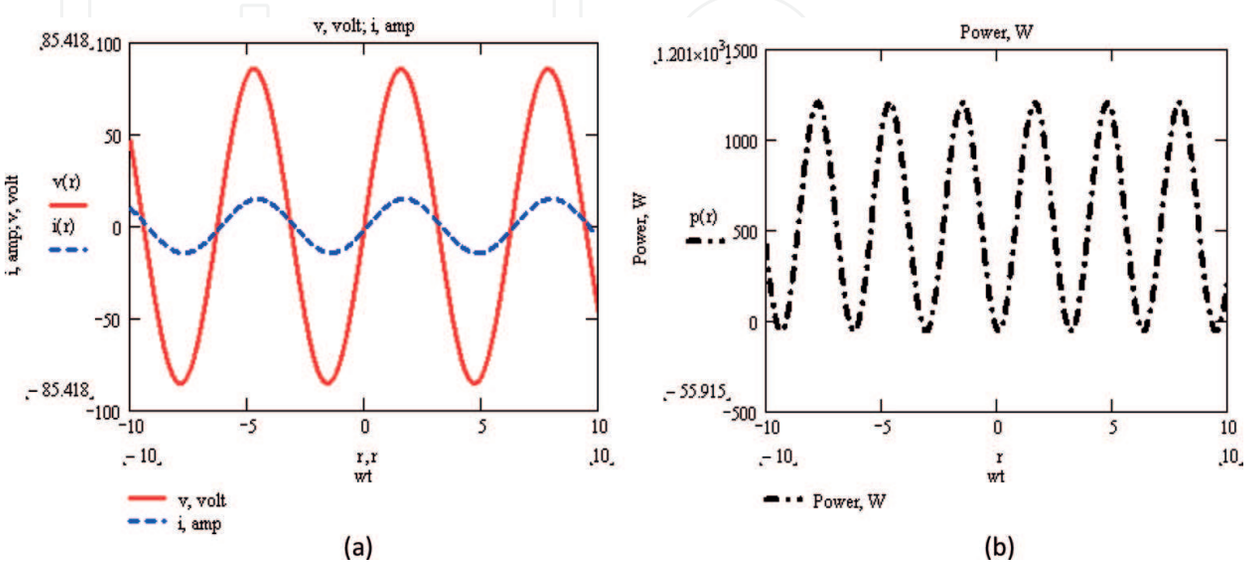

Figure 10. Time diagrams: (a) voltage and current and (b) power in a RC circuit amplifier.

$$p(t) = \frac{Vm.Im}{2}.\cos(\theta) - \frac{Vm.Im}{2}.\cos(2\omega - \theta) \quad (7)$$

The plots: The time diagram for current and voltage is plotted in **Figure 10(a)**. The time diagram for power is plotted in **Figure 10(b)**.

Power transfer: **Figure 10** shows that the instantaneous power is negative whenever the voltage and current are of opposite sign. However, as is illustrated in **Figure 10** that positive area of p(t) energy exceeds the negative area. Therefore, the average power is finite. Since the angle, θ, is small between current and voltage, the negative area of energy becomes very small. During the first quarter cycle (from 0° to 90°), the applied voltage rises from slightly negative value to a maximum, and the capacitor is receiving a charge. The power curve is positive during this period and represents energy stored in the capacitor. From 90° to 180°, the applied voltage is falling from maximum to slightly negative value, and the capacitor is discharging. The corresponding power curve is negative and represents energy returned to the circuit during this interval. The third quarter cycle represents a period of charging the capacitor, and the fourth quarter represents a discharge period. The induction losses are due to the thermal storage amount to 1.5% in comparison to the capacitive heating. Thus, induction losses cannot be avoided in any electrical circuit, but can be minimized.

7. Discussion

The following composite waves are generated due to the development of stresses and oscillations on a PV solar wall device with incident short wavelength electro-magnetic waves [1]: (i) due to the connected external electrical load and transmission of electrical energy wave; (ii) due to the exchange of viscous dissipation with air and the propagation of heat waves at longer wavelength; (iii) due to the thermal stress generation with propagation of heat waves, and elastic waves are transmitted in a PV solar wall device; (iv) due to the combination of stress development with heat waves, elastic waves, and applied external source of energy, and the fluid surface waves are propagated; and (v) due to the climate particle oscillations of wind and fan induced pressure, and applied external waves are propagated; in the absence of wind and fan pressure, thermosyphon-based oscillations are propagated due to the thermal buoyancy [18, 23].

Such as in an organ pipe, the sound waves can transmit with the combination of applied external source of energy and fluid surface waves. From the surrounding environment due to air-borne sound transmission, the sound waves are propagated. Due to various stresses and oscillations acting on a static particle body, the transmission of composite waves is generated. With the action of composite forces acting on a PV solar wall device, the developed stresses are classified as: (i) fundamental; (ii) internal; and (iii) external. Due to the presence of electromagnetic and gravitational forces of a solar system, the fundamental stresses are generated. Under the influence of fundamental stresses, internal stresses are generated with characterization of composition properties at chemical, atomic, and molecular level. With application of external source of energy such

as fan-based force used for active air ventilation in PV solar wall device, the external stresses are generated. With stress development due to the periodic force of expansion/compression, cooling/heating and night/day, the oscillations are assumed to be generated on the PV solar wall device. On a PV solar wall device, climate particle oscillations due to wind force are also transmitted. Due to the superposition of composite waves, the fluctuating forces are generated.

Resonance: The parallel and series cases of LCR circuit resonance are briefed here [8, 10]. With the aid of presented modeling and experimental data, the cases of resonance are visualized. For elastic waves transmission, the inductance force exists due to the mass of the mechanical system. The capacitance force exists due to the heat storage capacities of PV solar wall device (PV modules, air, and polystyrene filled plywood board). The polystyrene filled plywood board is vulnerable to heat stress of fire as soon as heat waves propagated with frequency matching with its latent heat of vaporization is achieved. Due to the thermal and fluid resistance in energy storage elements of the PV solar wall device, equivalent electrical analog resistance is developed. The parallel case of LCR resonance happens with fluid surface waves (RC) and heat waves (RC) in conjunction with inductance (L) due to the mass of PV solar wall device and resistance (R) due to temperatures of ambient air and ground surface. The series case of LCR resonance occurs with propagation of elastic waves of a PV solar wall device.

8. Conclusion

A study on solar energy conversion and noise characterization in photovoltaic devices with ventilation is performed. The noise interference and characterization as per speed of a composite wave are presented. The sources of noise waves (sun, light, sound, heat, electricity, fluid, and fire) are described depending on their speed of noise interference. Noise measurement equations and their units are coined. The power systems are classified as per source signals of solar power, electric power, light power, sound power, heat power, fluid power, and fire power. The noise filters for filtering noise from power systems are defined with examples. The experimental results along with results of the simulation model for noise filtering for a PV device are presented. Some noise unit examples for an air duct exposed to solar radiation are illustrated. A phenomenon of photovoltaic amplification for a pair of photovoltaic modules connected to a potentiometer is explained. The time plots of power function were used to support and devise noise measurement expressions and noise characterization in a power system as per speed of a wave.

Author details

Himanshu Dehra

Address all correspondence to: anshu_dehra@hotmail.com

Egis Group, Gurugram, Haryana, India

References

[1] Dehra H. A unified theory for stresses and oscillations. In: Proc. CAA Conf., Montréal 2007 Canada, Canadian Acoustics. Vol. 35(3). 2007. pp. 132-133

[2] Dehra H. Power transfer and inductance in a star connected 3-phase RC circuit amplifier. In: Proc. AIChE 2008 Spring Meeting, New Orleans, LA, USA. Session 96a. 2008. 7 p

[3] Dehra H. The noise scales and their units. In: Proc. CAA Conf., Vancouver 2008 Canada, Canadian Acoustics. Vol. 36(3). 2008. pp. 78-79

[4] Dehra H. A benchmark solution for interference of noise waves. In: Proc. AIChE Spring 2009; Tampa, FL, USA; April 26-30, Session 67c. 2009. 4 p

[5] Dehra H. Solar energy absorbers. In: Manyala R editor. Chapter 6 in Solar Collectors and Panels, Theory and Applications. Intech Publication; 2010. pp. 111-134

[6] Dehra H. A theory of acoustics in solar energy. Natural Resources. 2013;**4**(**1A**):116-120

[7] Dehra H. A slide rule for noise measurement. In: 10th International Conference on Sustainable Energy Technologies (SET 2011); Istanbul, Turkey; September 4-7. 2011. 5 p

[8] Dehra H. A novel theory of psychoacoustics on noise sources, noise measurements and noise filters. In: Proc. NoiseCon16 Conf.; 13-15 June; Providence, Rhode Island, USA. 2016. pp. 933-942

[9] Dehra H. On sources and measurement units of noise. In: Proc. International Conference on Innovation, Management and Industrial Engineering (IMIE 2016); 05-07 August 2016; Kurume, Fukuoka, Japan; 2016. pp. 219-227. ISSN: 2412-0170

[10] Dehra H. Acoustic filters. In: Romano VA, Duval AS, editors. Chapter 5 in Ventilation: Types, Standards and Problems. New York, USA: Nova Science Publishers; 2011. 245 pp. ISBN: 978-1-62618-281-3

[11] Dehra H. A paradigm for characterization and checking of a human noise behavior. In: WASET Proceedings of 19th International Conference on Psychological and Brain Sciences; May 11-12, 2017; Montréal, Canada. pp. 317-325. http://waset.org/publications/10007615

[12] Dehra H. Photovoltaic solar wall: 2-D numerical modeling and experimental testing under fan induced hybrid ventilation. In: Proceedings of the IEEE International Conference on Energy Efficient Technologies for Sustainability, April 7-8. IEEE Xplore, ISBN: 978-1-4673-9925-8; 2016. pp. 668-676

[13] Dehra H. A multi-parametric PV solar wall device. In: Proceedings of IEEE International Conference on Power, Control, Signals and Instrumentation Engineering (ICPCSI-2017), 978-1-5386-0814-2/17/$31.00 ©2017 IEEE, Chennai, India on 21-22 Sep 2017

[14] Dehra H. Characterization of noise in power systems. In: Proceedings of IEEE International Conference on Power Energy, Environment & Intelligent Control (PEEIC2018), 978-1-5386-2341-1/18/$31.00 ©2018 IEEE, Greater Noida, India on April 13-14, 2018. pp. 321-330

[15] Dehra H. A guide for signal processing of sensors and transducers. In: Proc. AIChE 2009 Spring Meeting; Tampa, FL, USA. 2009. Session 6b

[16] Dehra H. A numerical and experimental study for generation of electric and thermal power with photovoltaic modules embedded in building façade [submitted/unpublished Ph.D. thesis]. Montréal, Québec, Canada: Department of Building, Civil and Environmental Engineering, Concordia University; August 2004

[17] Dehra H. The effect of heat and thermal storage capacities of photovoltaic duct wall on co-generation of electric and thermal power. In: AIChE. 2007 Spring Meeting; April 22-26; Houston, Texas, USA. Session 36a. 2007. 9 p

[18] Dehra H. The entropy matrix generated exergy model for a photovoltaic heat exchanger under critical operating conditions. International Journal of Exergy. 2008;**5**(2):132-149

[19] Dehra H. A two dimensional thermal network model for a photovoltaic solar wall. Solar Energy. 2009;**83**(**11**):1933-1942

[20] Dehra H. Electrical and thermal characteristics of a photovoltaic solar wall with passive and active ventilation through a room. International Journal of Energy and Power Engineering. 2017;**11**(5):514-522. http://waset.org/publications/10007024

[21] Dehra H. An investigation on energy performance assessment of a photovoltaic solar wall under buoyancy-induced and fan-assisted ventilation system. Applied Energy. 2017;**191**(1):55-74

[22] Dehra H. A combined solar photovoltaic distributed energy source appliance. Natural Resources. 2011;**2**:75-86

[23] Dehra H. A mathematical model of a solar air thermosyphon integrated with building envelope. International Journal of Thermal Sciences. 2016;**102**:210-227

IntechOpen